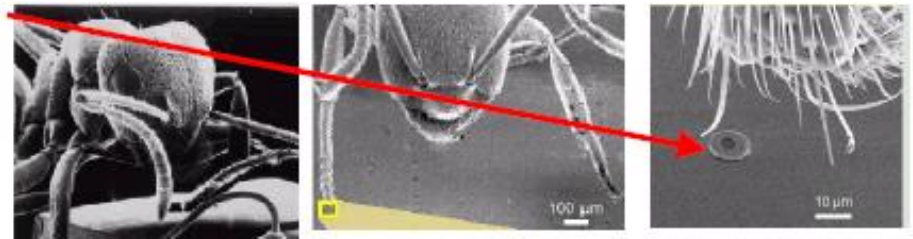


NANOMATERIALS AND NANOTECHNOLOGIES.

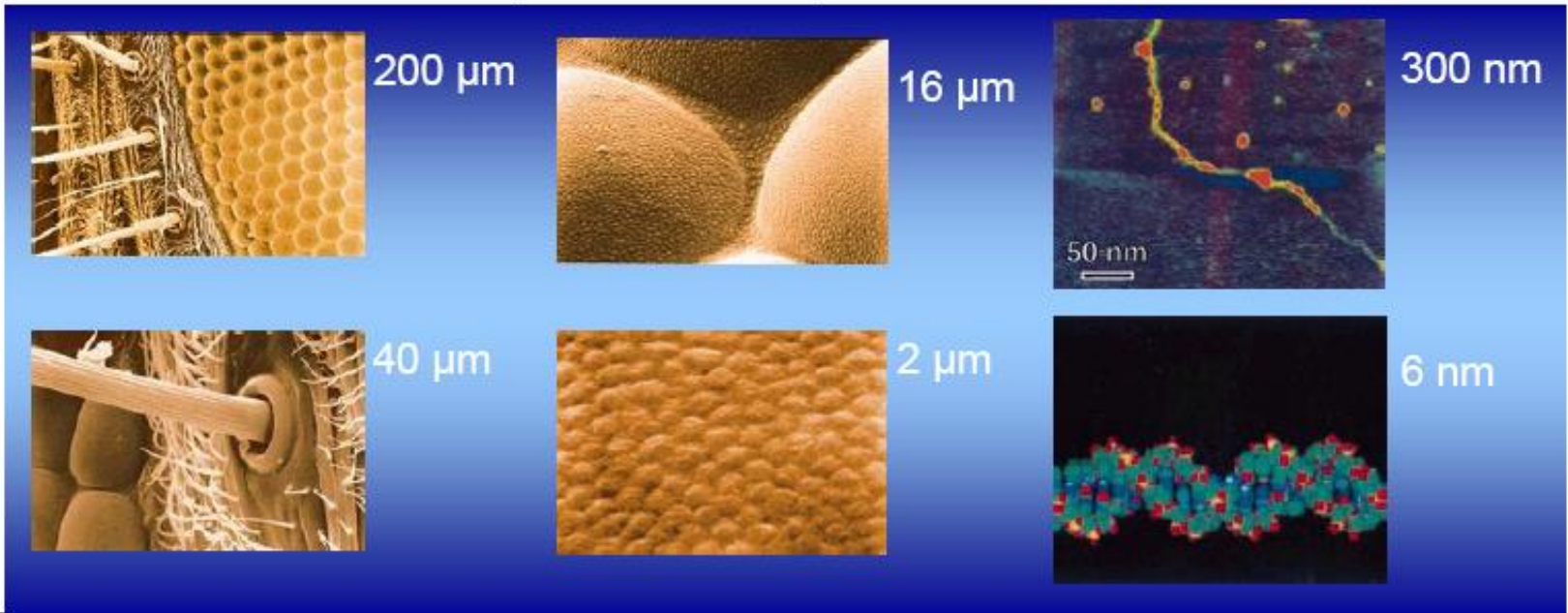
The journey into the nano-cosmos (1)

Ant and diode laser (VCSEL)



A fly's eye in the microcosm
(200 μm to 2 μm)

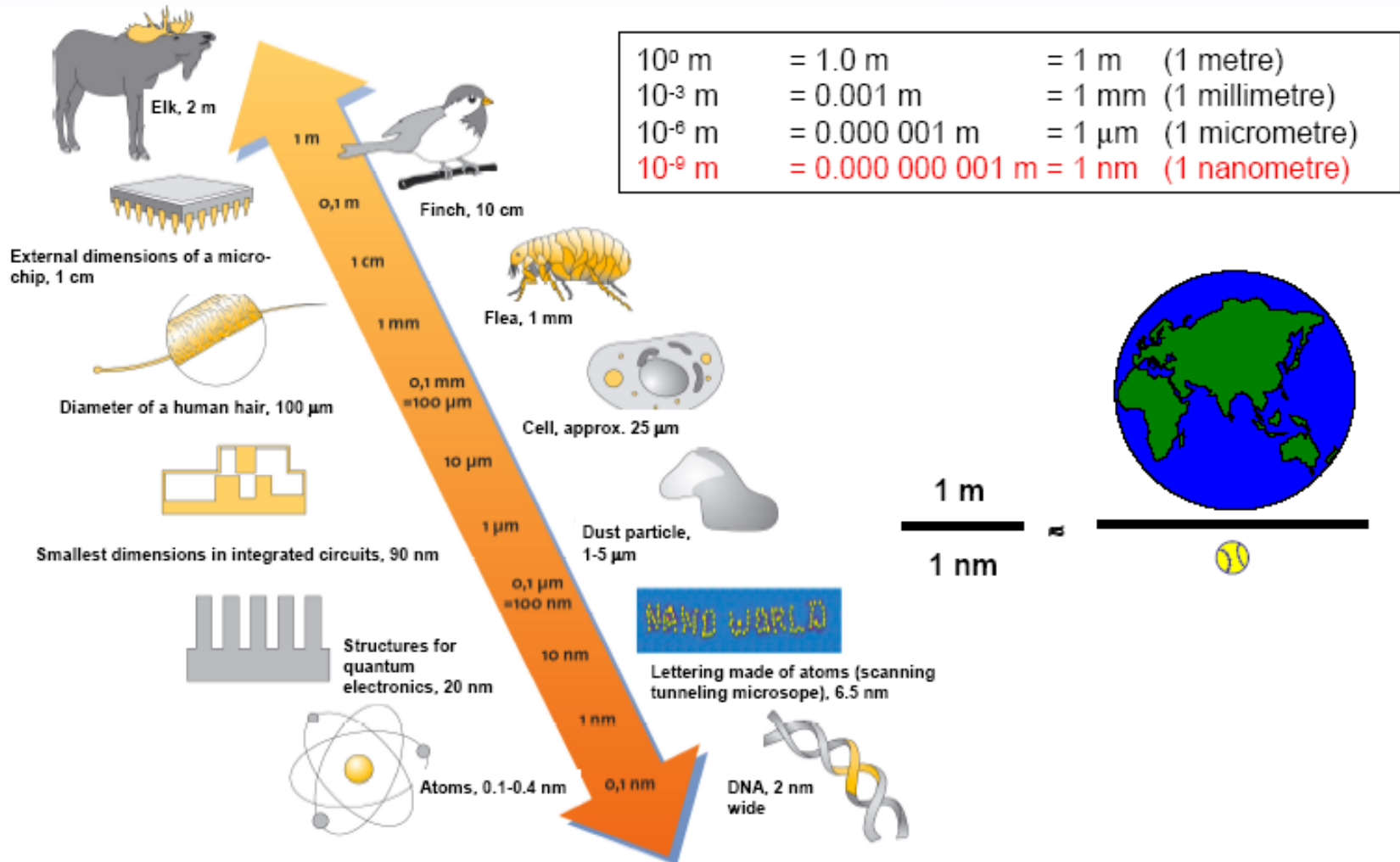
DNA in the nano-cosmos (300 nm to 6 nm)

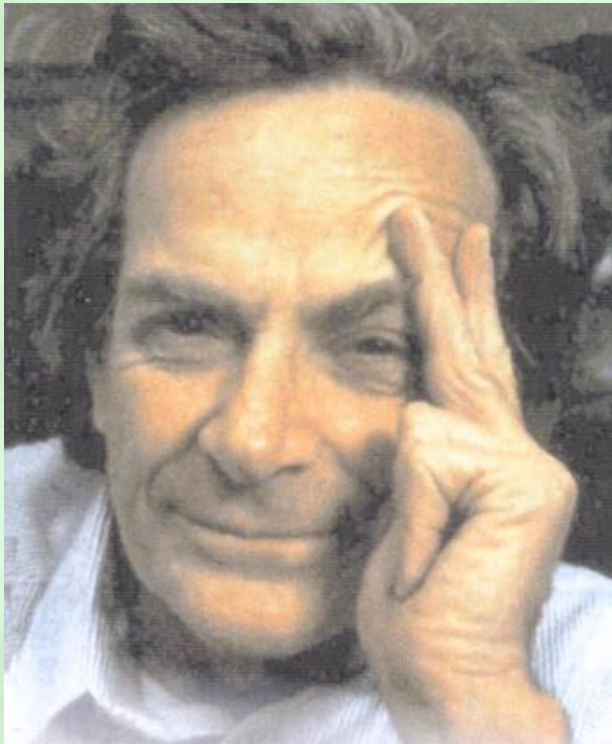


The journey into the nano-cosmos (2)

Size relationships

The journey into the nano-cosmos I: Scientific and technical principles





→ || ← 60 nm

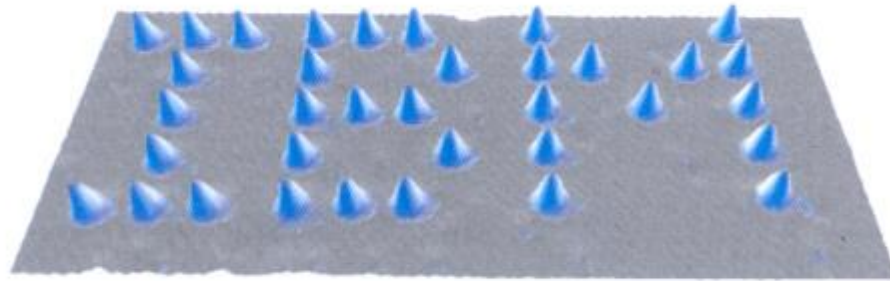
As soon as I mention this, people tell me about miniaturization, and how far it has progressed today. They tell me about electric motors that are the size of the nail on your small finger. And there is a device on the market, they tell me, by which you can write the Lord's Prayer on the head of a pin. But that's nothing; that's the most primitive, halting step in the direction I intend to discuss. It is a staggeringly small world that is below. In the year 2000, when they look back at this age, they will wonder why it was not until the year 1960 that anybody began seriously to move in this direction.

← || → 400 nm

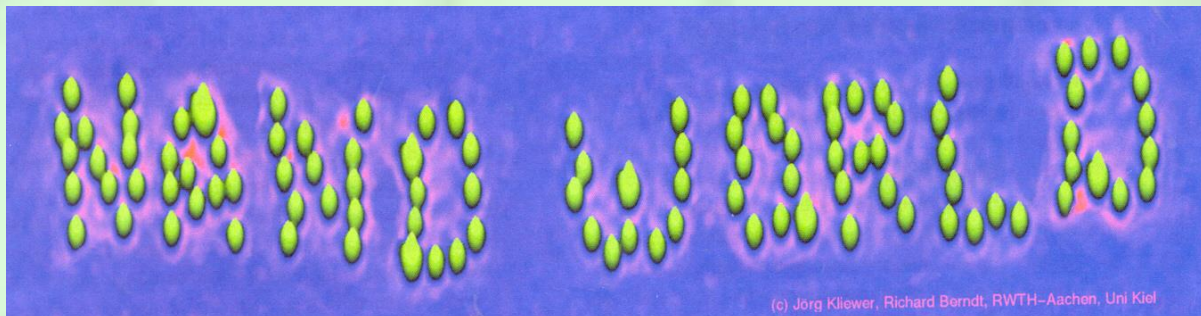
Richard P. Feynman, 1960

Richard Feynman: „There's plenty of room at the bottom”

1990



Logo IBM (Donald Eigler i Erhard Schweizer)



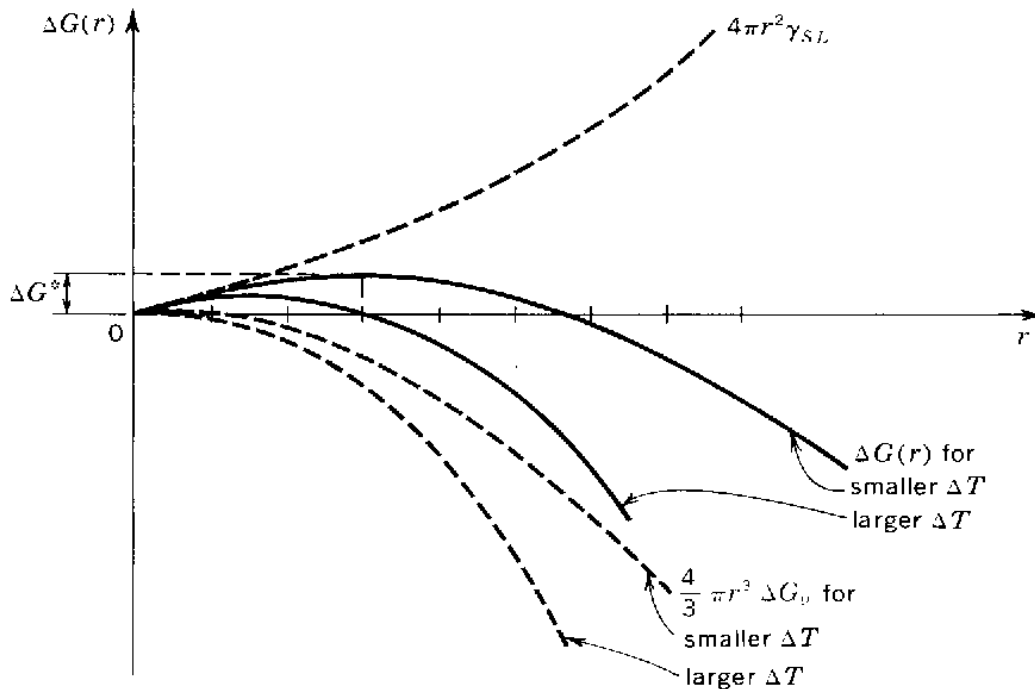
(c) Jörg Klewer, Richard Berndt, RWTH-Aachen, Uni Kiel

NANO WORLD

For nucleation, the critical size has always been of the order of nm!

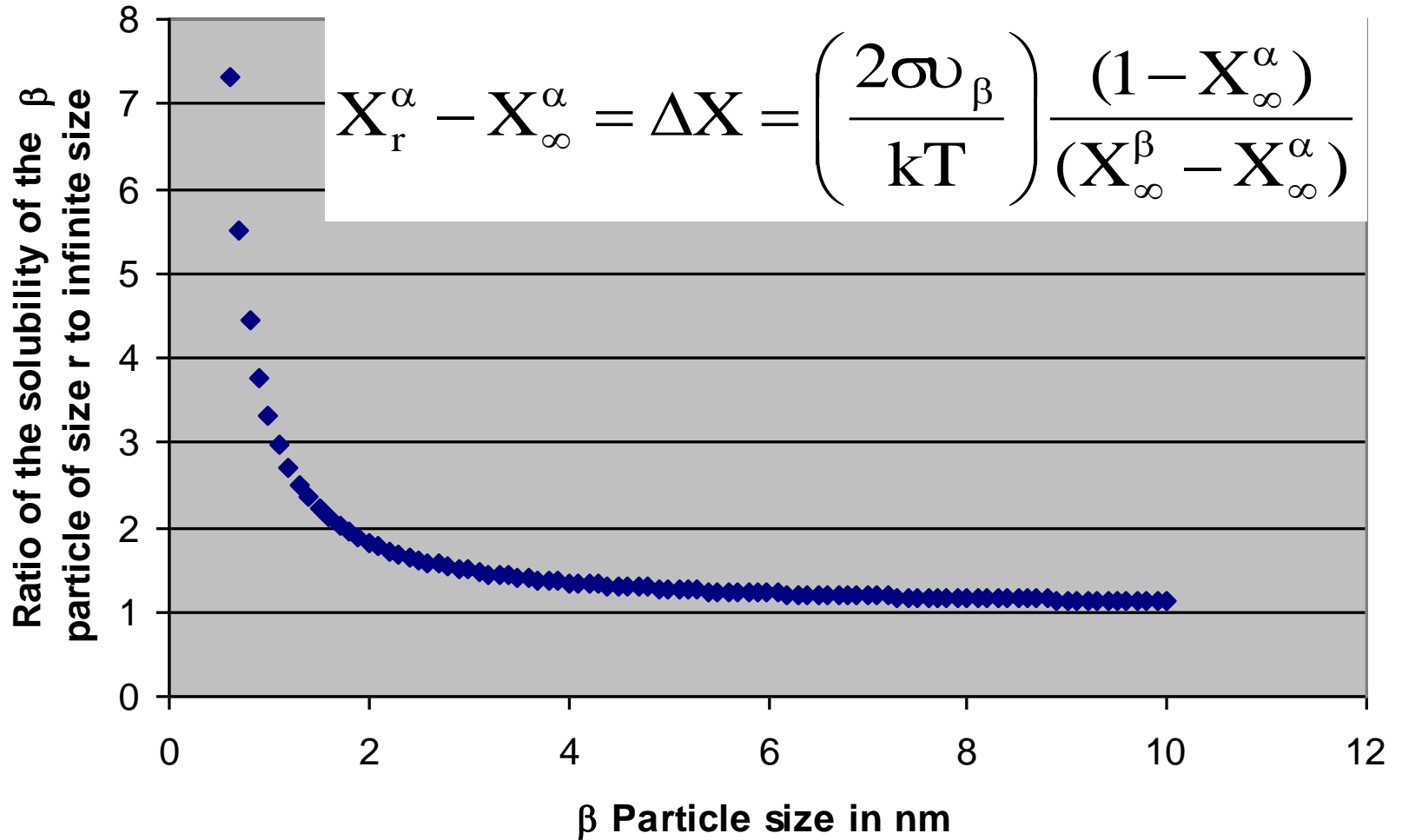
$$\Delta G = \frac{4\pi}{3} r^3 \cdot \Delta G_V + 4\pi r^2 \cdot \gamma_{SL}$$

$$r^* = -\frac{2\gamma_{SL}}{\Delta G_V}$$



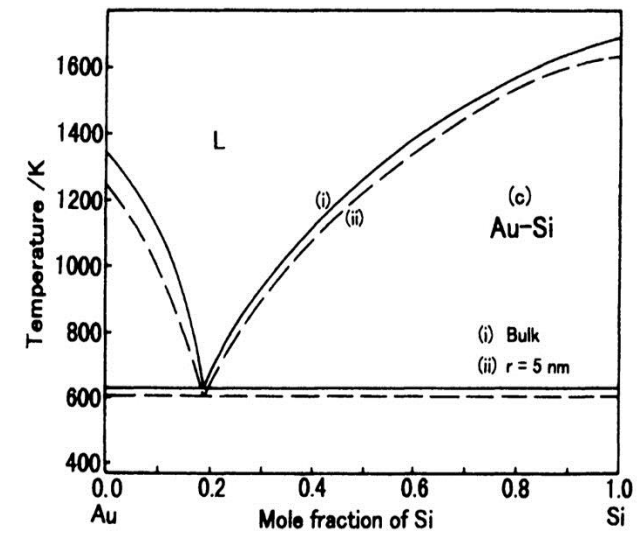
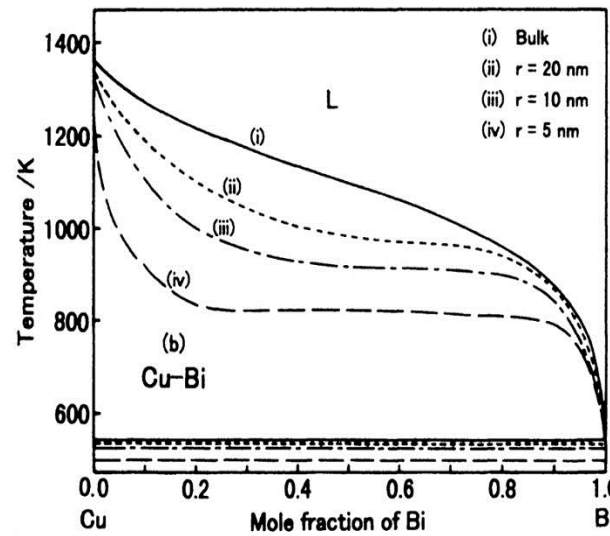
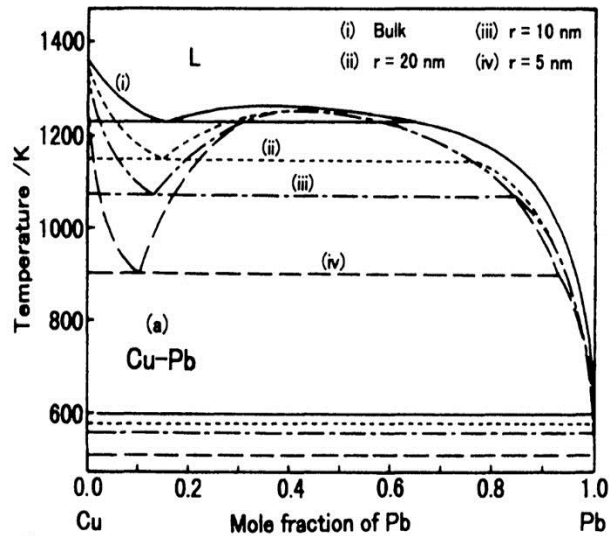
Plot of the free-energy terms making up $\Delta G(r)$ and of $\Delta G(r)$ for a small and large undercooling. The critical radius r^ is at the maximum in $\Delta G(r)$ and decreases as ΔT increases.*

Solubility of a β Particle as function of its size



$${}^{ex}G_m = \sum_{i=1}^2 \sum_{j=i+1}^3 \left[\frac{x_i x_j}{V_{i,j} V_{j,i}} \right] \cdot {}^{ex}G_{i,j}$$

$$G_m = x_A {}^0G_A + x_{Bi} {}^0G_{Bi} + x_B {}^0G_B$$



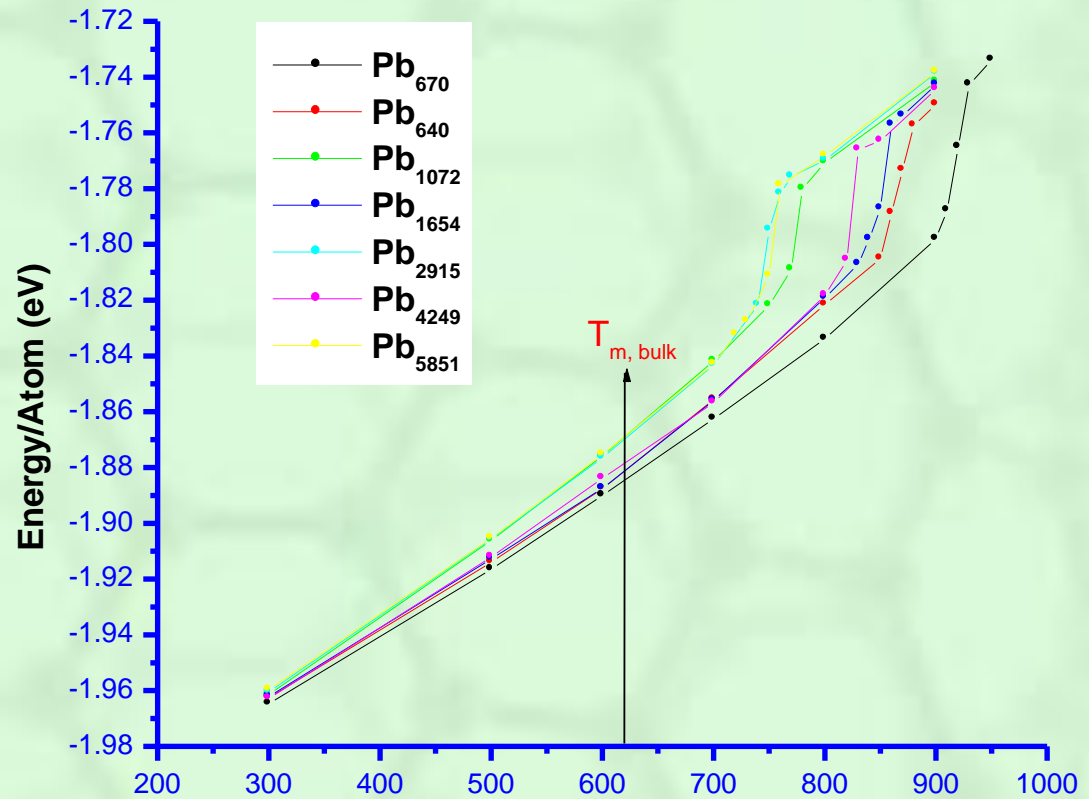
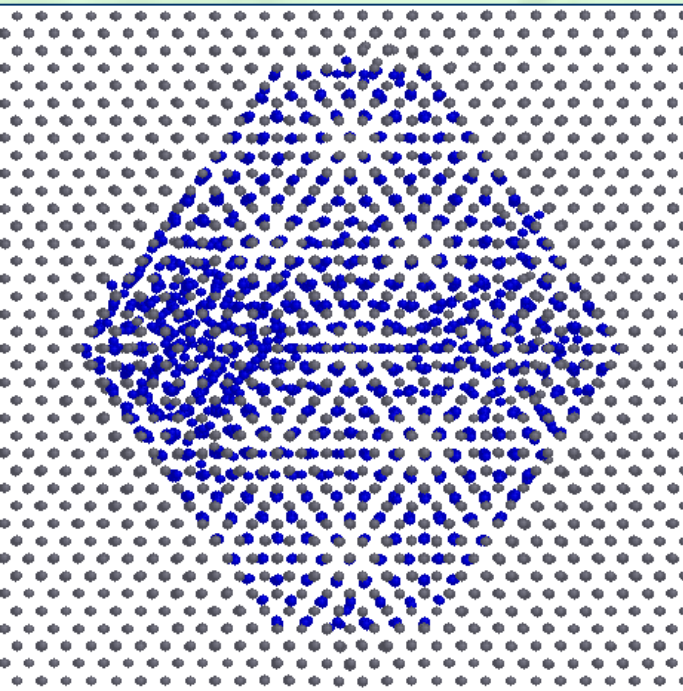
T. Tanaka, S. Hara: „Thermodynamic Evaluation of Binary Phase Diagrams of Small Particle Systems”, Z. Metallk. 92 (2001) 5, 467-472.

$$V_{i,j} = \frac{1+x_i-x_j}{2} \quad V_{j,i} = \frac{1+x_j-x_i}{2}$$

But...!

● Pb

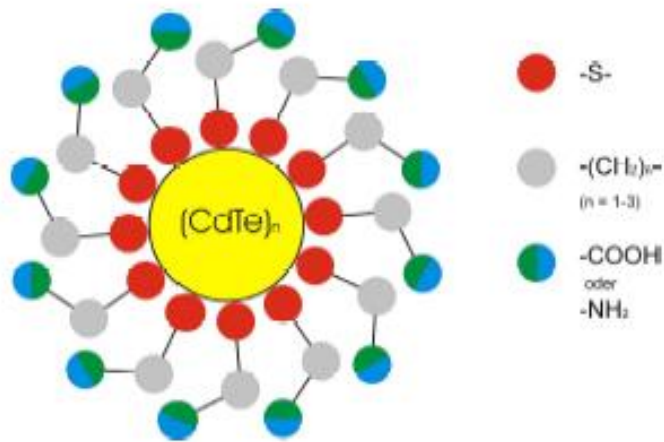
● Al



The melting of embedded Pb in Al occurs over a continuous range of temperatures. It is as though there is a two phase equilibrium between Pb(L) atoms at the surface and Pb(S) atoms in the interior. After Zhan Shi, Ph.D Thesis , CMU, 2004

Properties of different-sized nano-particles

Nano-particles are tiny crystals: the smaller they are, the more they behave **like a molecule**




Schematic of a CdTe nano-particle with stabilising shell

CdSe nano-particles in solution (1.5 - 4.0 nm)



Fluorescence depending on the particle size



2 nm  5 nm

Paul Mulvaney, MRS Bulletin, Dec. 2001, p.1009

Au Atom: ~0,1 nm (1Å), colorless

Au clusters: < 1nm, nonmetallic, orange

Au nanocrystallites: 3 - 30 nm, metallic, transparent / red

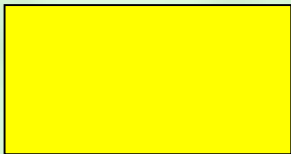
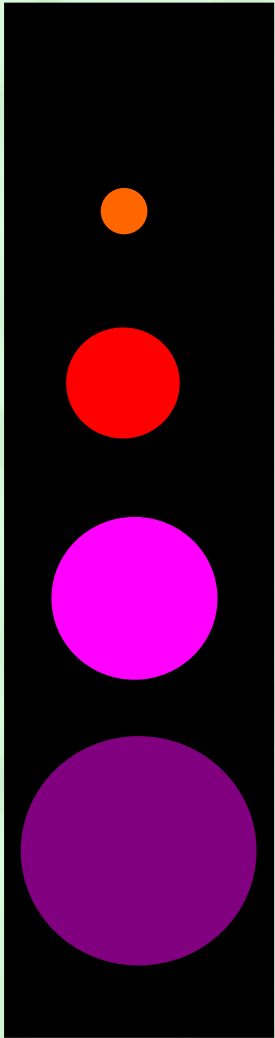
Au particles: 30 - 500 nm, metallic, transparent / turbid

crimson -> blue

M. Faraday, Philos. Trans. R. Soc. London, 147 (1857) 145-181

Gold leaf can be beaten to thicknesses of 1/278000 of an inch (around 90 nm). Such films are continuous and green in transmission. Further thinning with KCN gives ruby red films.

Chemical means to finely divided gold. Also deflagration of gold wires to produce ruby red particles. Chemically indistinguishable from gold.



Au bulk: golden color!

*Paul Mulvaney,
MRS Bulletin,
Dec. 2001, p.1009*

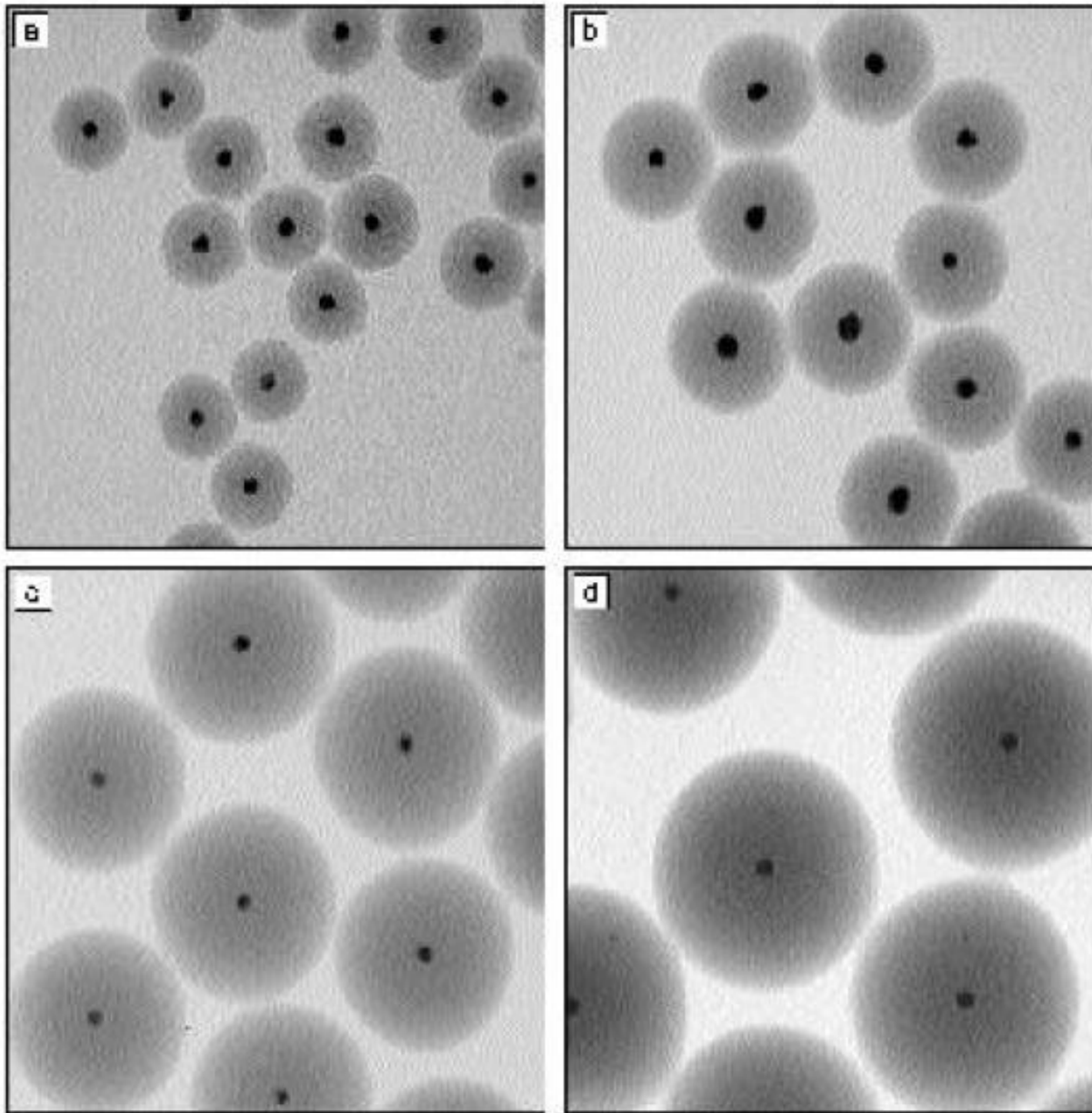


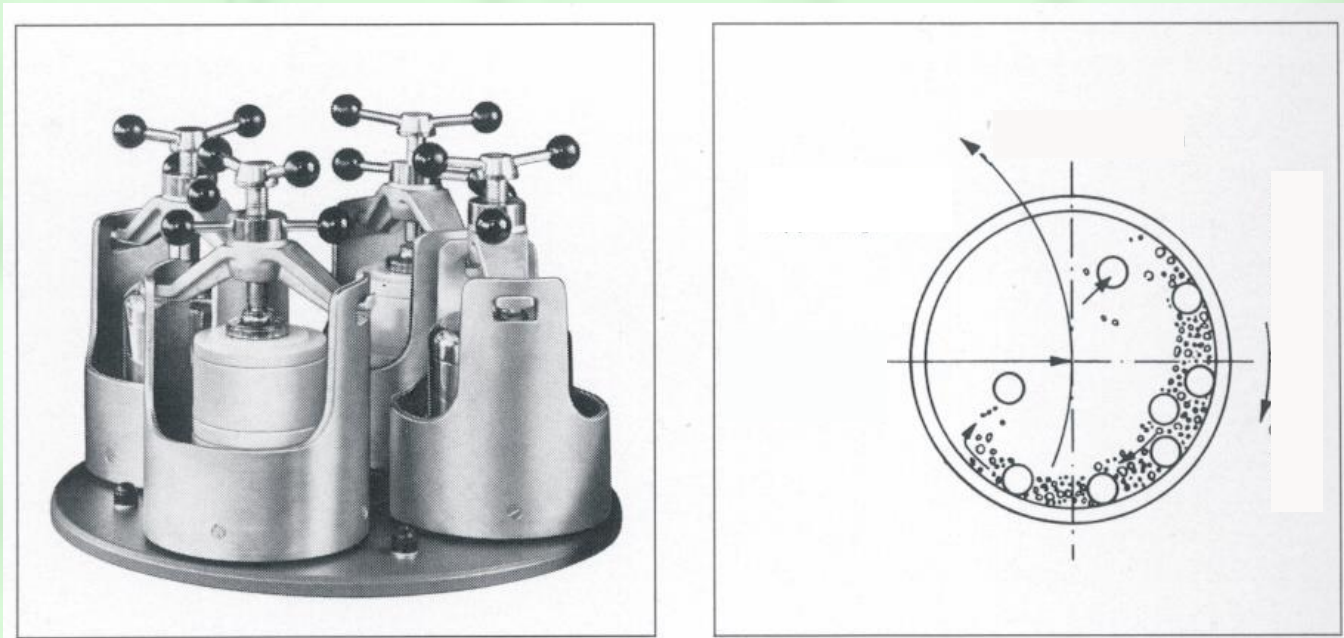
Figure 4. (a)–(d) Electron micrographs of silica-coated 15-nm gold particles with various shell thicknesses.

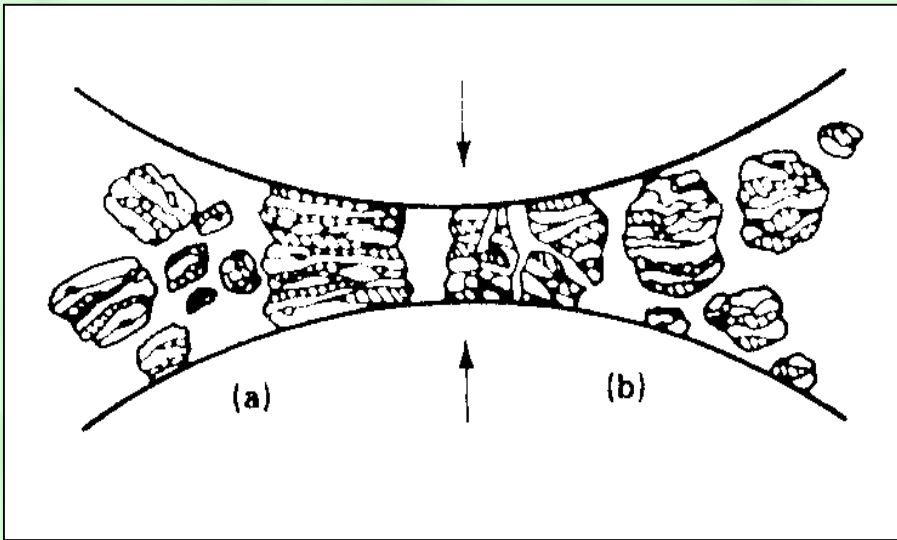
in the
limit of
very small
spacings
and
a gold volume
fraction 50%,
the film spectrum
is almost identical
to that
of the bulk
gold thin film ¹²

**NANOMATERIALS CAN BE
PRODUCED USING TWO BASIC
TECHNOLOGIES:**

- **TOP - DOWN CAN BE REALIZED BY:**

- CRUSHING IN BALL MILLS.

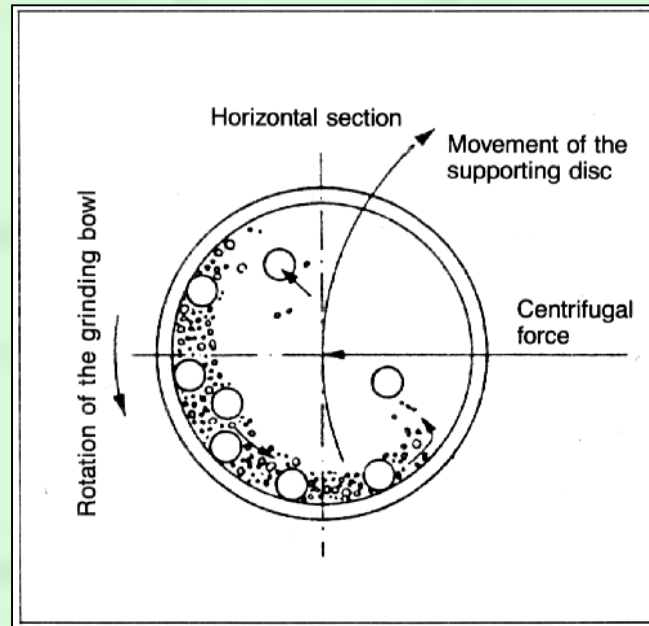




Scheme of mechanical alloying process

a) welding

b) fracturing

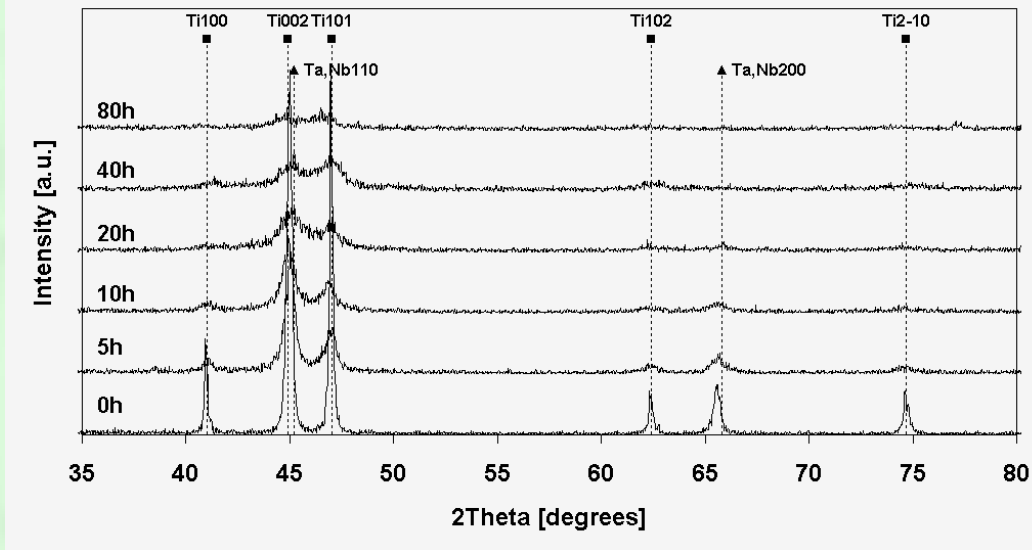


Planetary mill Fritsch Pulverisette P/4

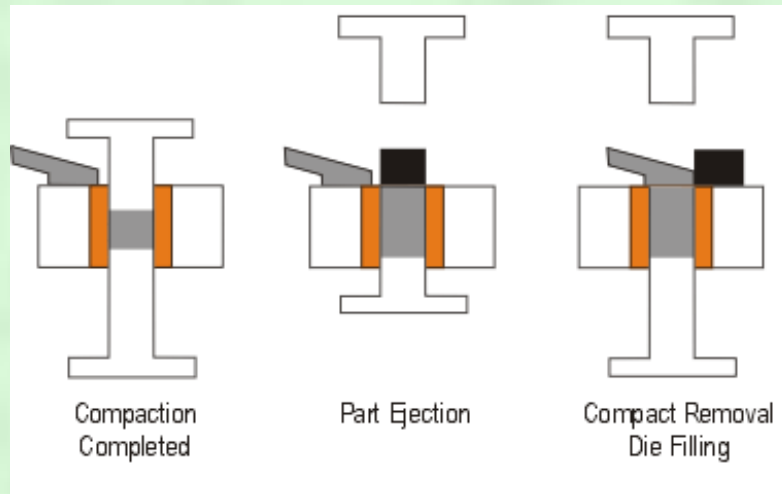
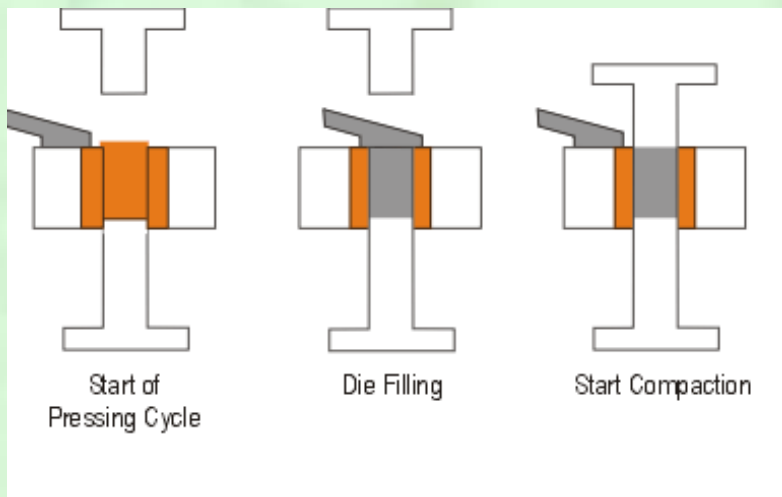
and scheme of ball
movement during
mechanical alloying
process

Table 2 Microhardness of Ti, TiNb and TiTa Nb samples ball milled and uniaxially hot pressed

Sample	Ball milled powder μHV_{20}	Uniaxially hot pressed μHV_{20}
Ti	1029 \pm 149	1037 \pm 100
TiNb	822 \pm 40	773 \pm 69
TiTa Nb	786 \pm 92	610 \pm 89



Set of diffraction pattern of Ti-10Ta-10Nb alloy after different milling time.

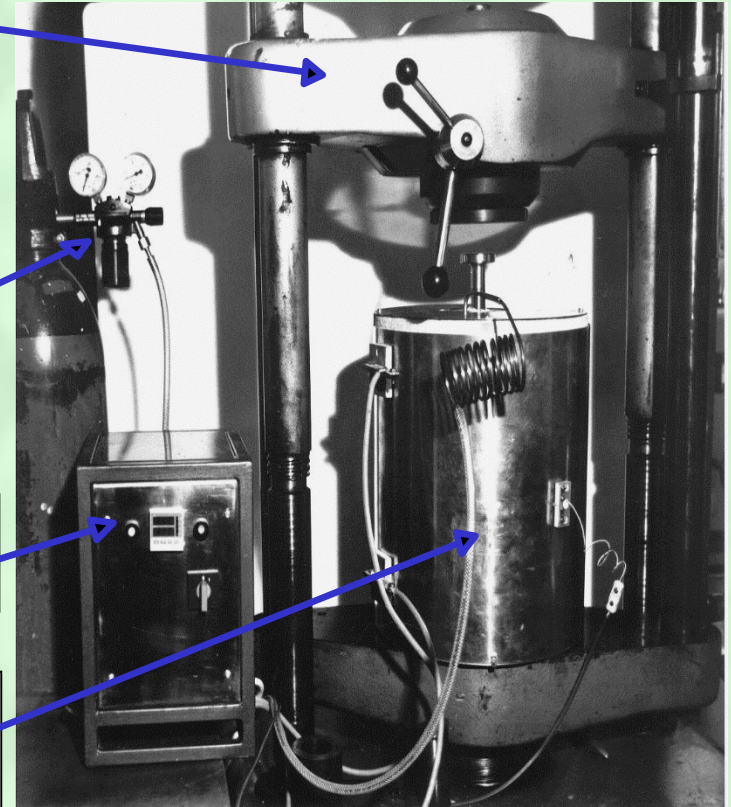


Hydraulic press
Type VEB-
WPM 400 kN

Argon
supplied
system

Temperature
regulator

Furnace and
graphite
mould

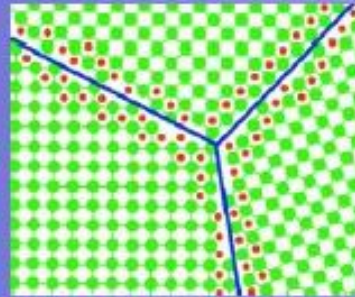


Scheme of the applied uni-axial hot pressing

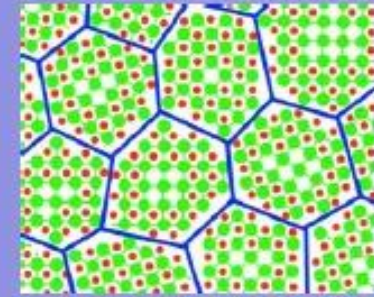
Photograph of the applied hot pressing device

✓ Nano-Powders

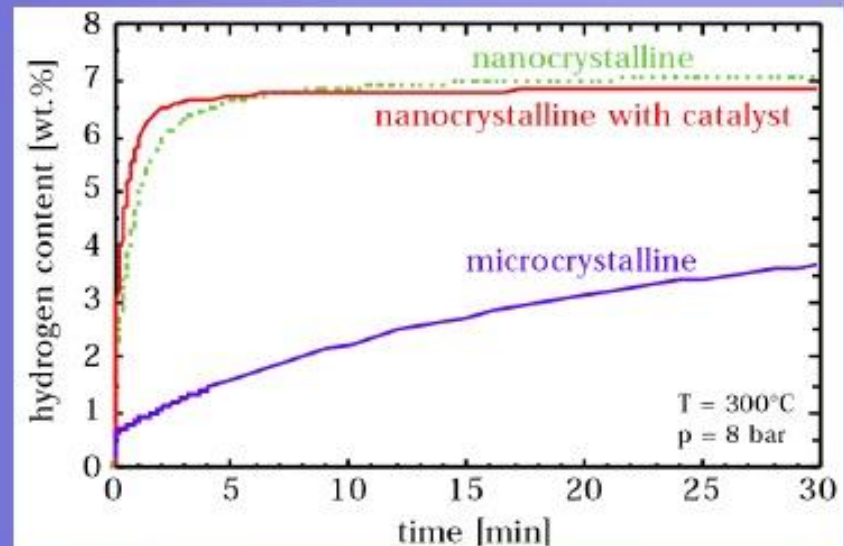
- + Enhanced diffusion and kinetics through grain boundaries
- + Low desorption temperature
- Surface contamination
- Commercially non usable technique and environmental risks



Coarse grained structure

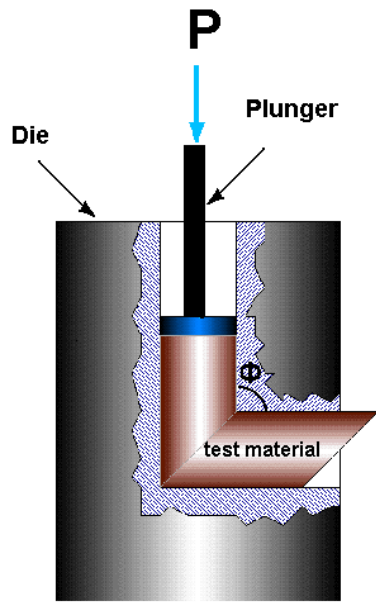


Nanocrystals

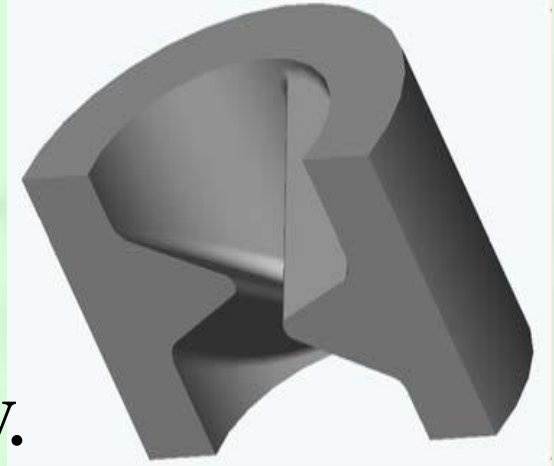


T.Klassen, et al., Z. Metallkd., 94, 610 (2003)

⇒ Bulk NMs

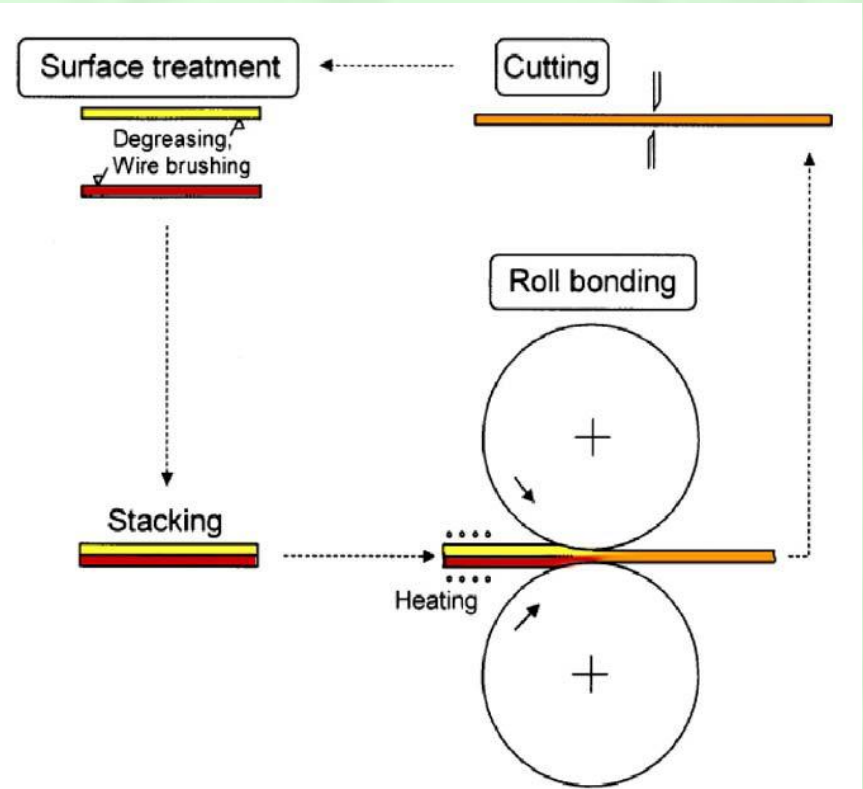
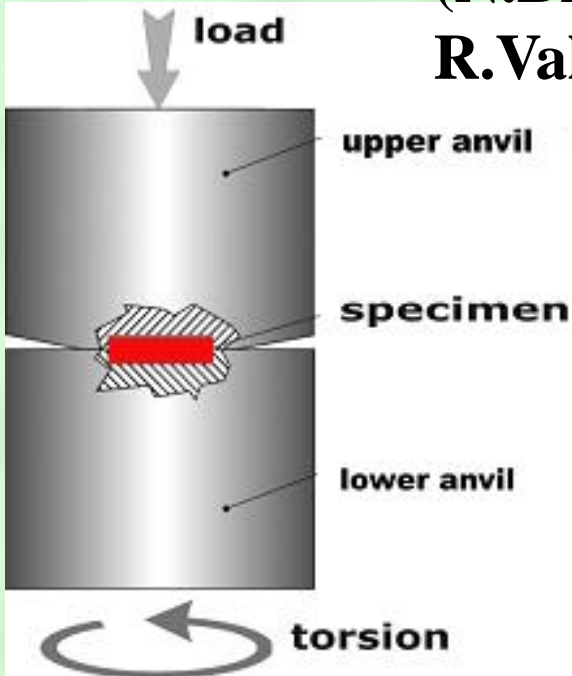


Equal Channel Angular Pressing (V. Segal, R. Valiev)

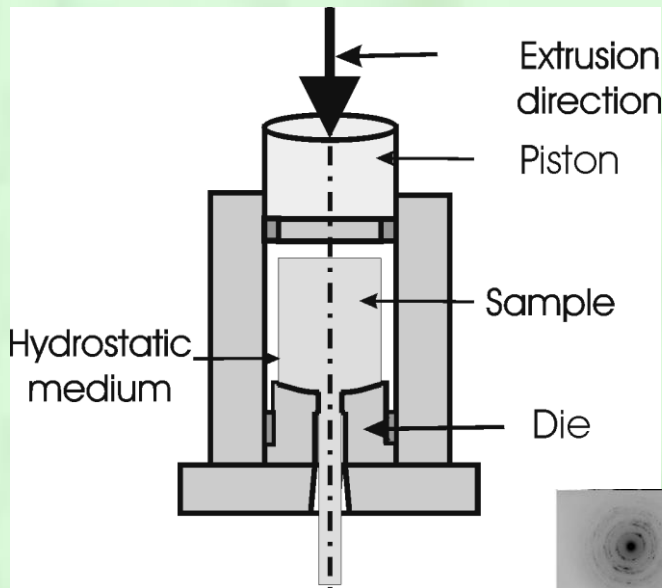


Torsional Extrusion (V. Varyukhin)

High Pressure Torsion (N. Bridgman, R. Valiev)

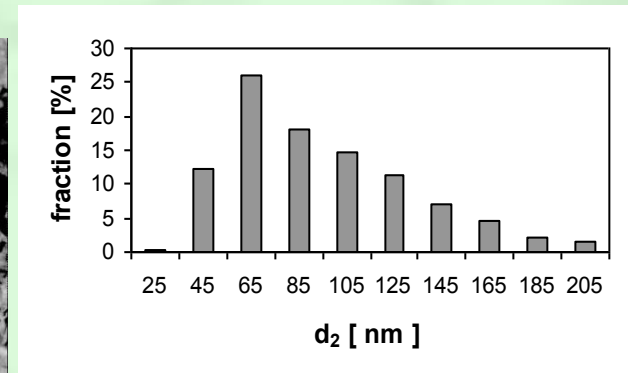
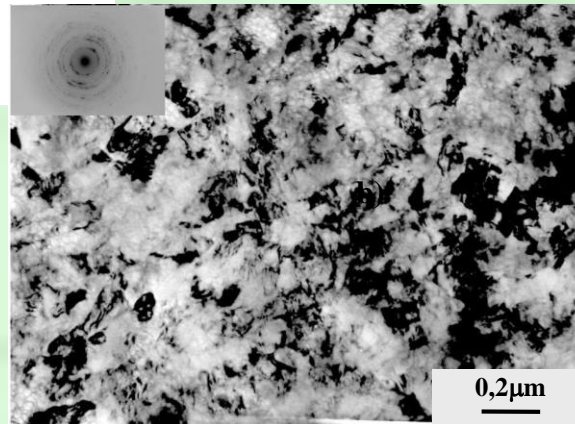


Vaccum. Roll Bonding (N. Tsuji)



Scheme of the hydrostatic extrusion processing

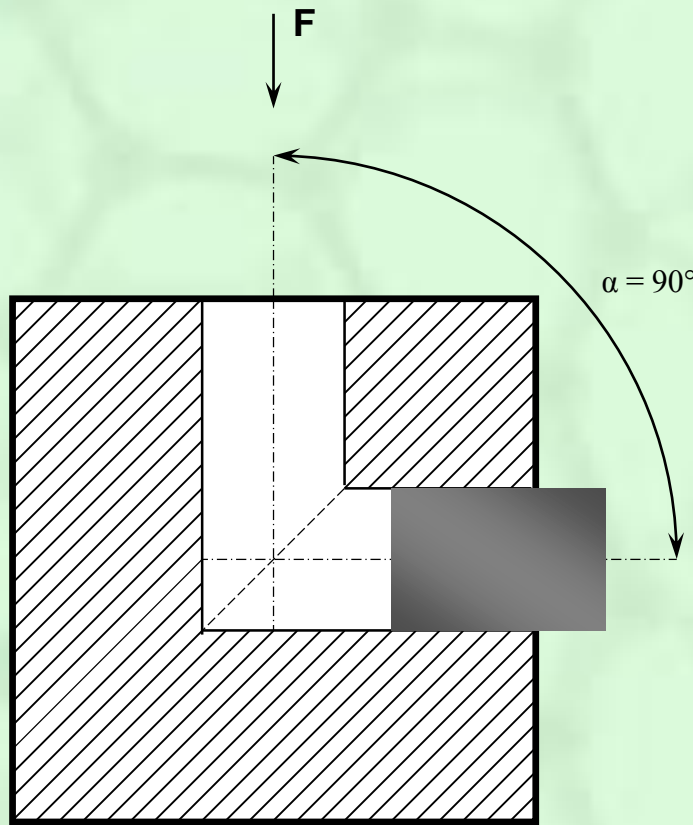
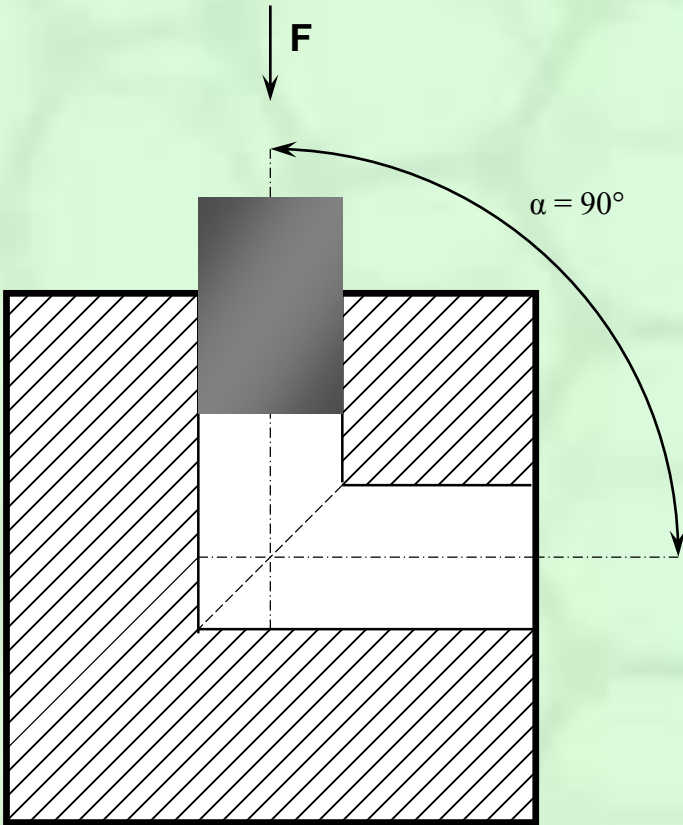
a)



$E(d_2) = 87$ [nm]
 $SD(d_2) = 42,9$ [nm]
 $C_v(d_2) = 0,5$

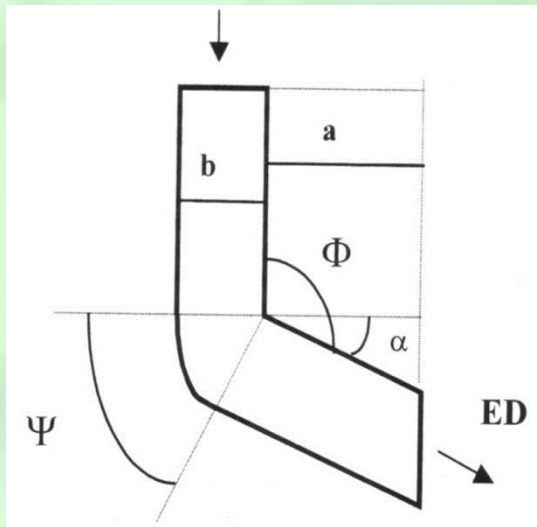
TEM micrograph (a) and grain size distribution (b) of Ti after hydrostatic extrusion (d_2 - equivalent diameter of grain size, $E(d_2)$ - mean equivalent diameter of grain size, $SD(d_2)$ -standard deviation, $C_v(d_2)$ -variation coefficient

(EQUAL-CHANNEL ANGULAR PRESSING)



(EQUAL-CHANNEL ANGULAR PRESSING)

$$\varepsilon_N = N * [2 * ctg(\phi / 2 + \psi / 2) + \psi * \sin^{-1}(\phi / 2 + \psi / 2)] / \sqrt{3}$$



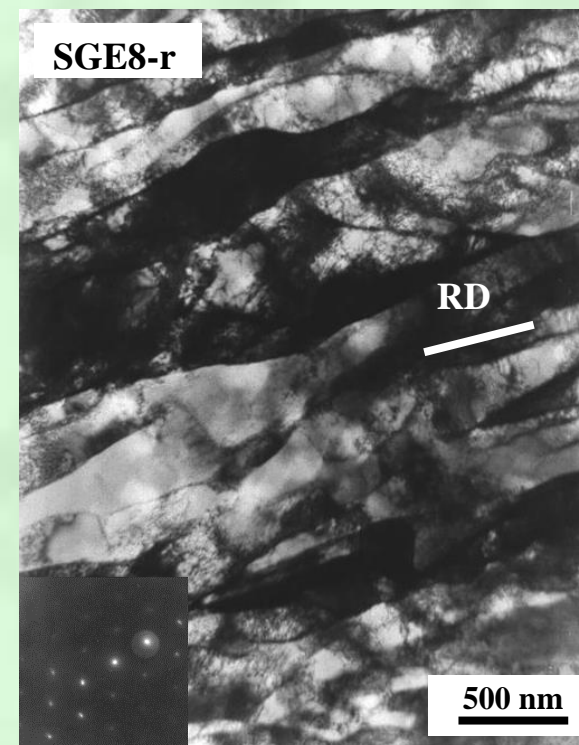
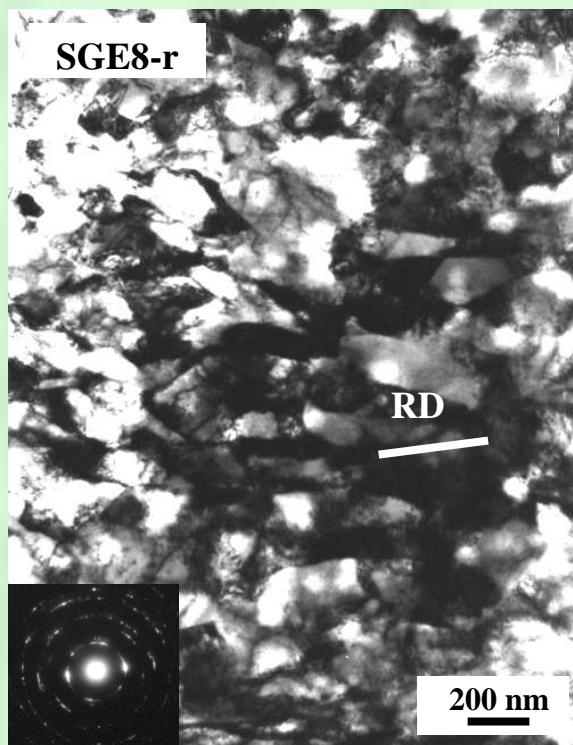
$$\Phi = 90^\circ + \alpha$$

$$\Psi = 90^\circ - \alpha$$

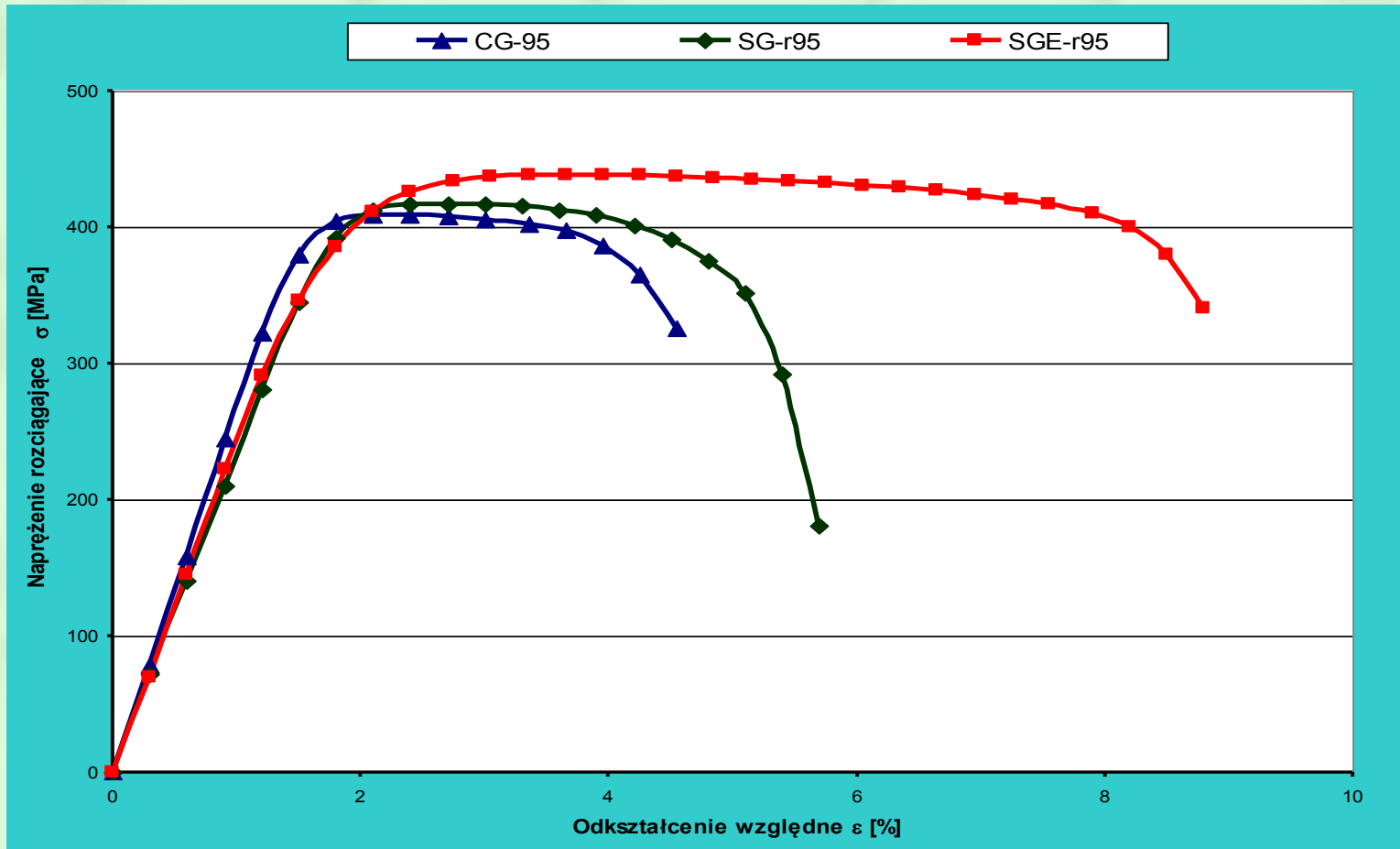
$$\alpha = 0$$

$$\varepsilon_N = N * 0,9069$$

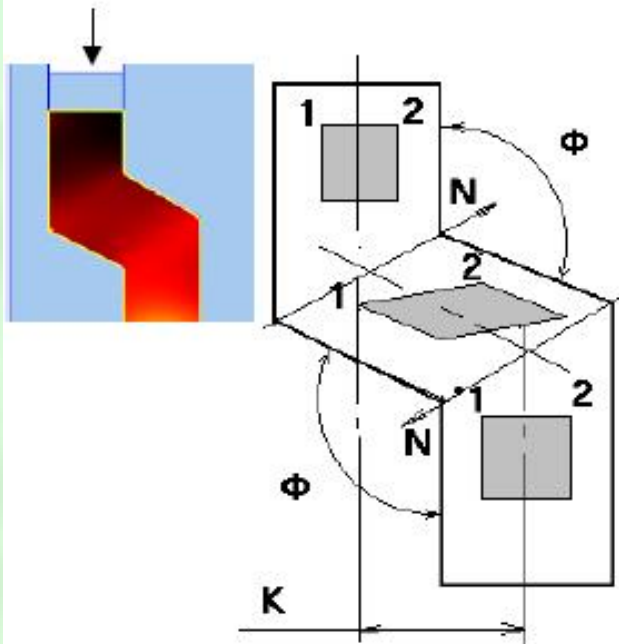
TEM MICROSTRUCTURES



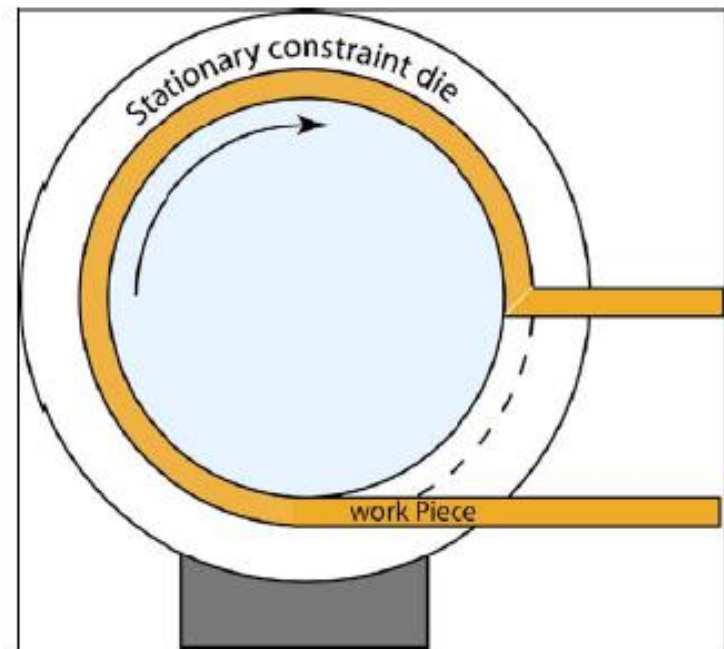
Mechanical properties tensile strength



New modifications of ECA pressing

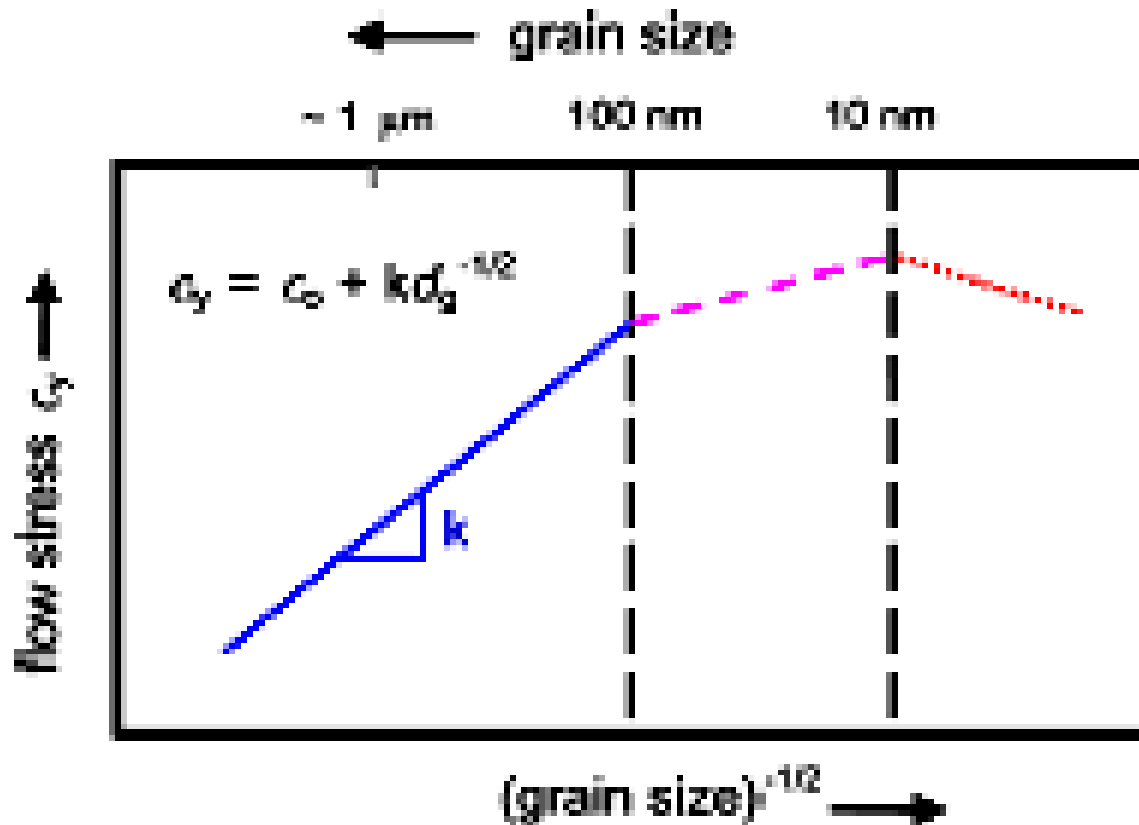


ECAP with parallel channels



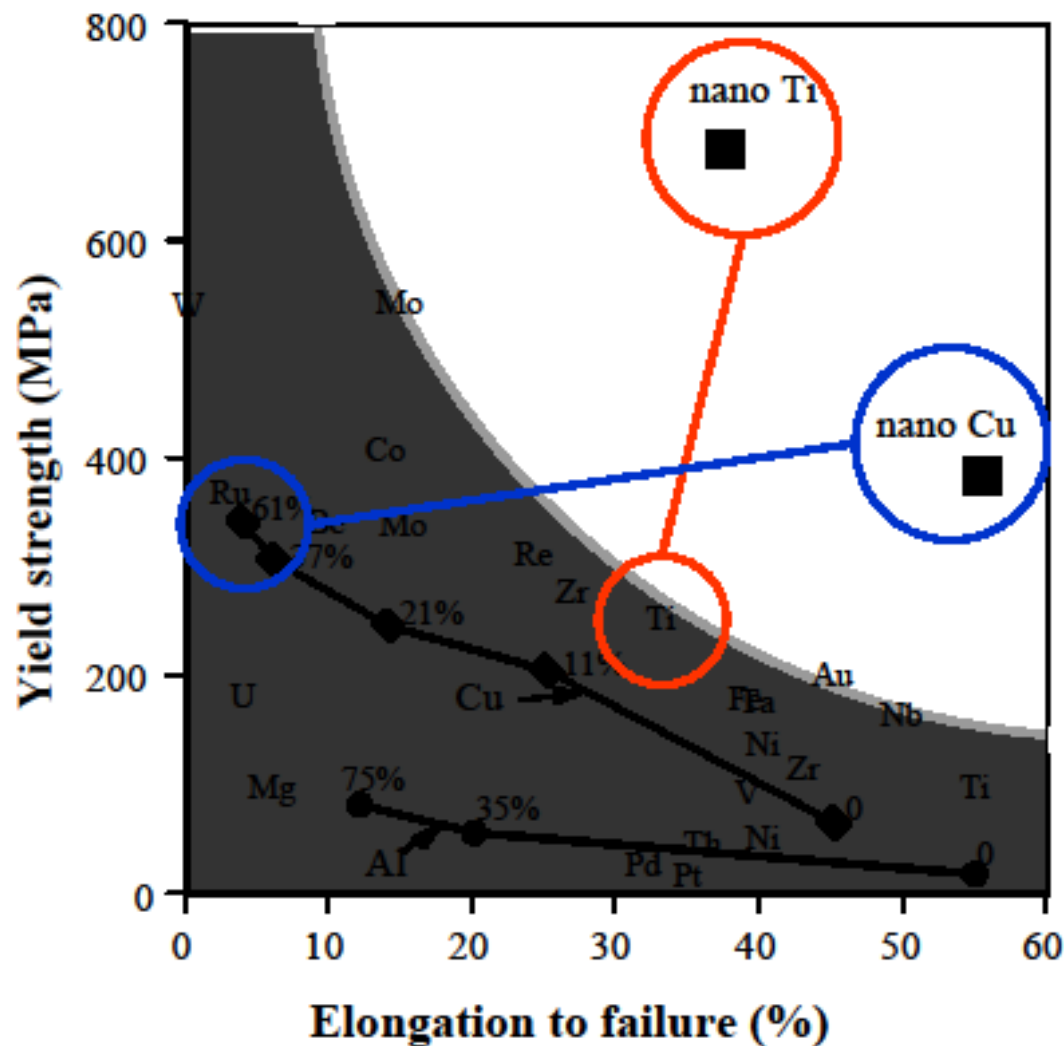
ECAP-Conform

RZ Valiev and TG Langdon, *Progr. Mater.Sci.*,2006

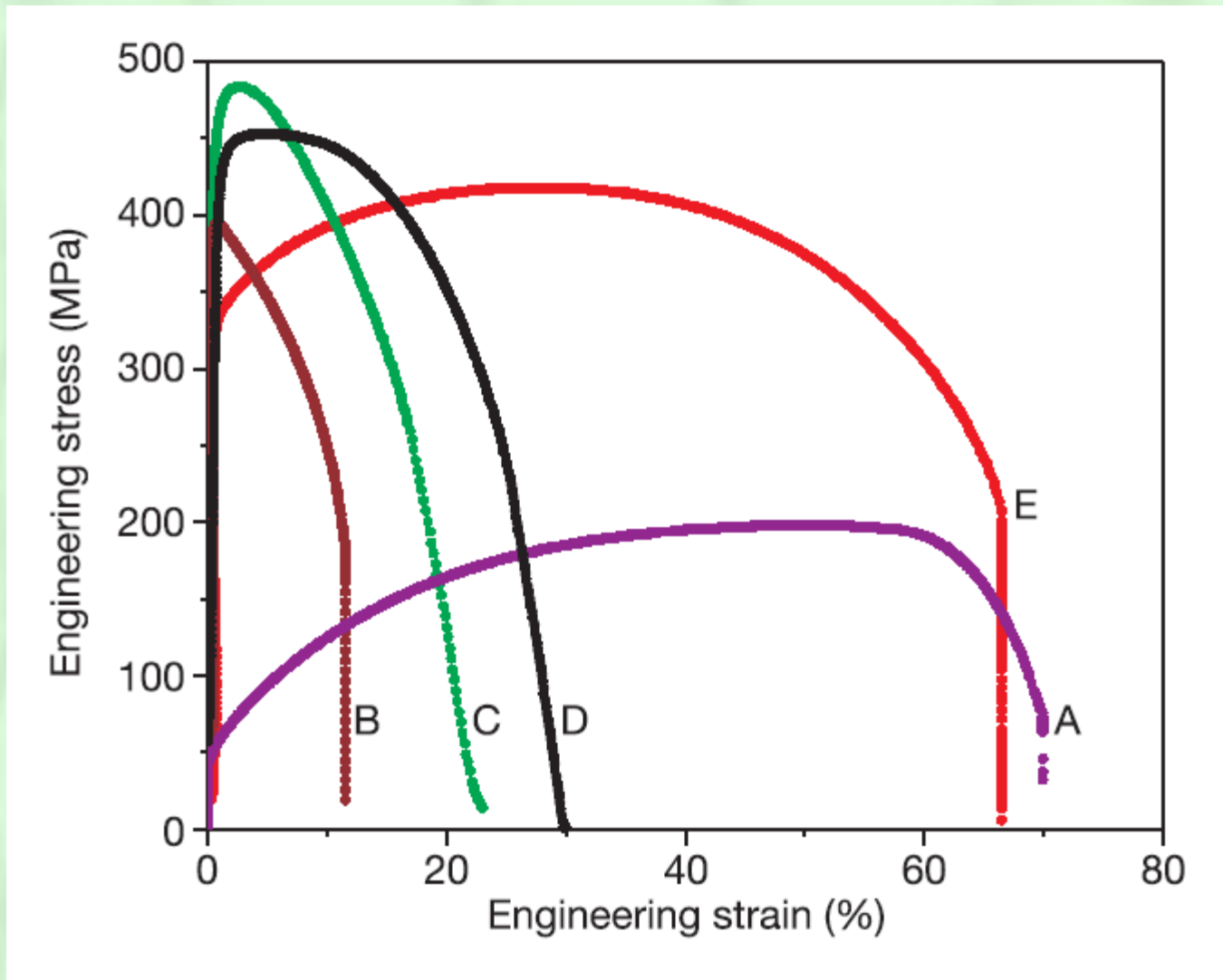


Yield stress as a function of grain size ($-1/2$) in micro and nano range for alloys and metals (after Kumar Acta mat. 2003 str.5747)

Advanced mechanical properties by SPD

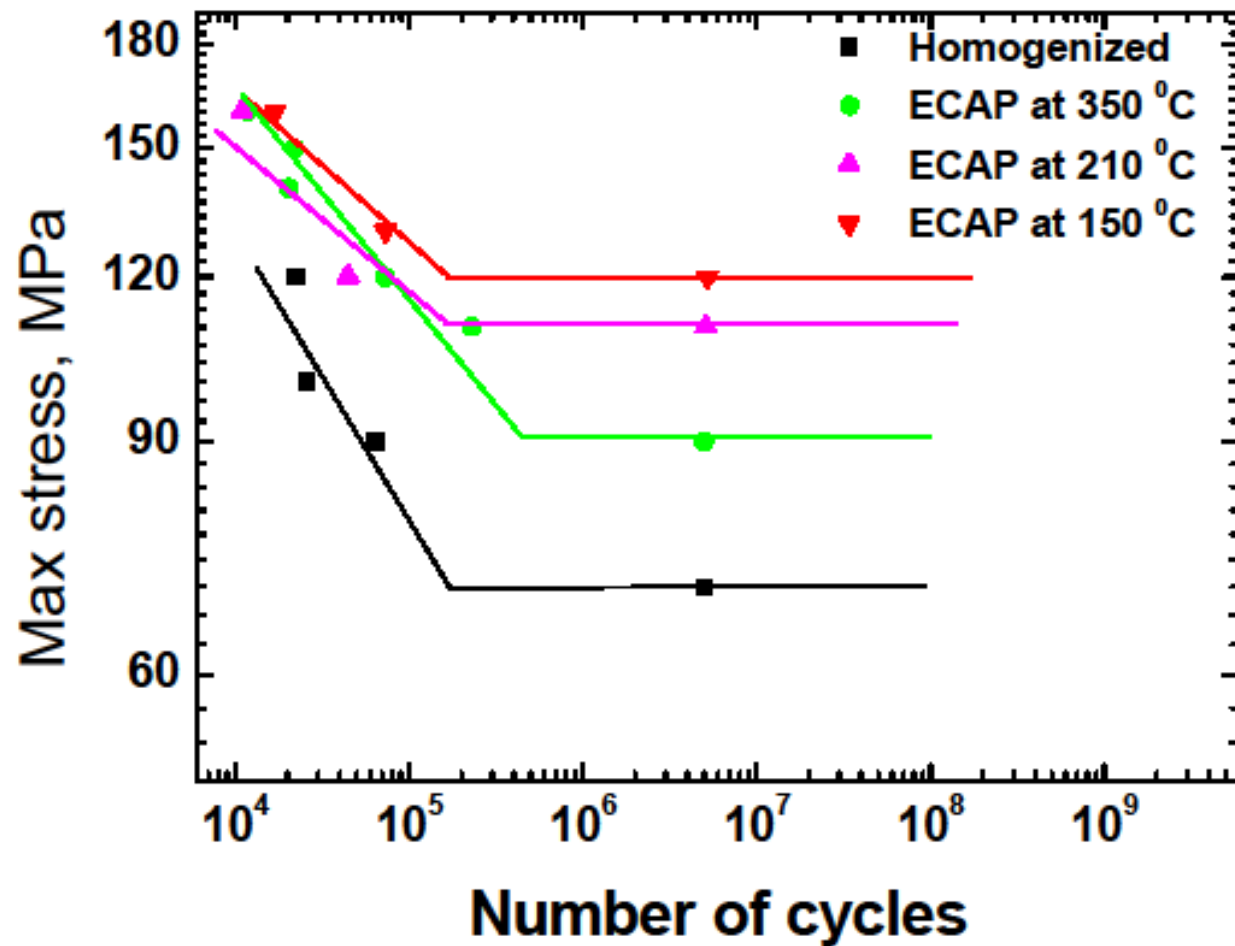


**Cu99,9
9**



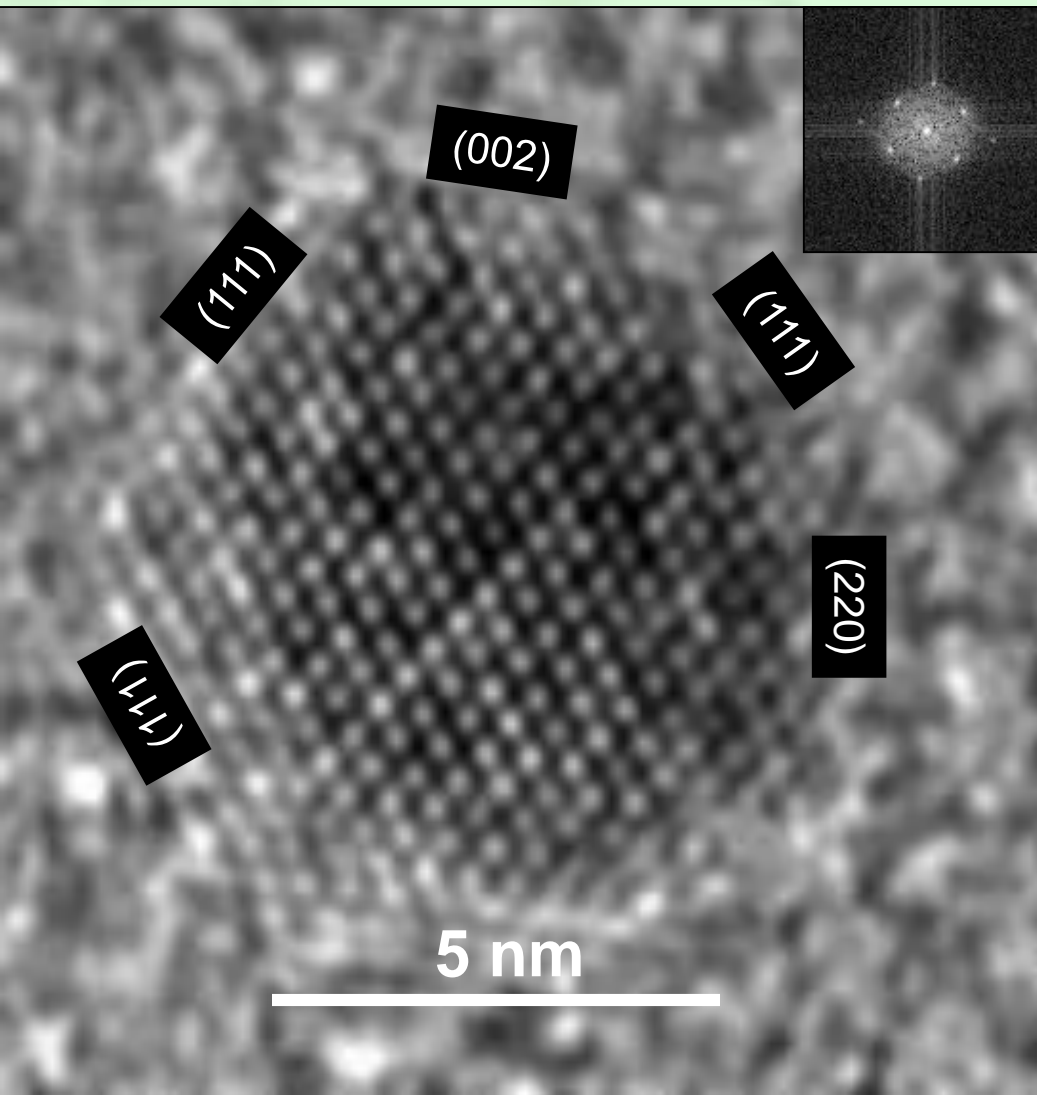
**High Strength and High Ductility of SPD Nanomaterials Y.Wang,
M.Chen, F.Zhou, En Ma, Nature 419, 912-915 (2002)**

Enhanced Fatigue Strength in ECAPed Mg-Al AM 60 alloy

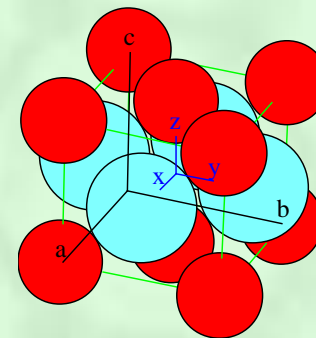
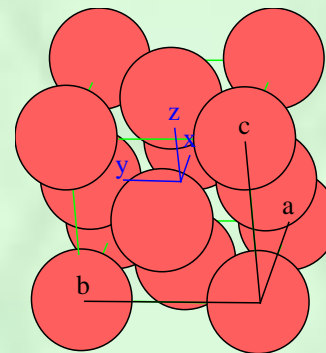


O. Kulyasova (USATU) et al., M. Zehetbauer et al. (Univ. Vienna) (2008)

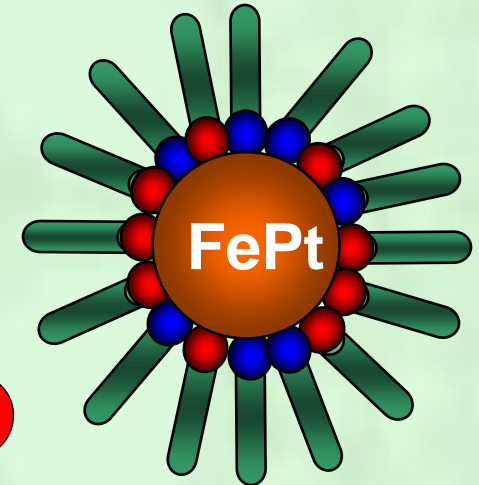
FePt Nanoparticles



fcc disordered

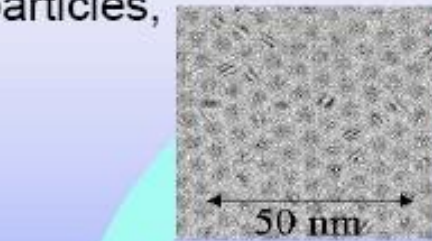


L1₀

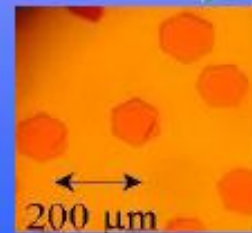
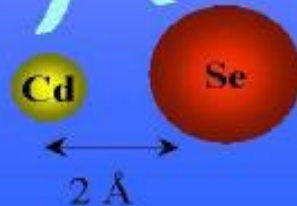
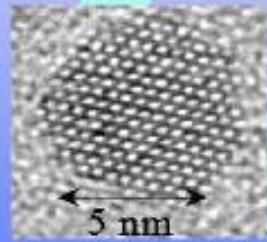
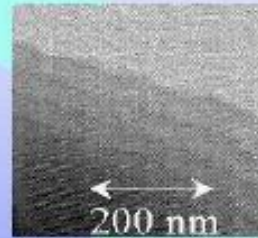


Surface structures of nano-particles: from the atom to the super-crystal

Cd and Se
atoms form
nano-particles,
...



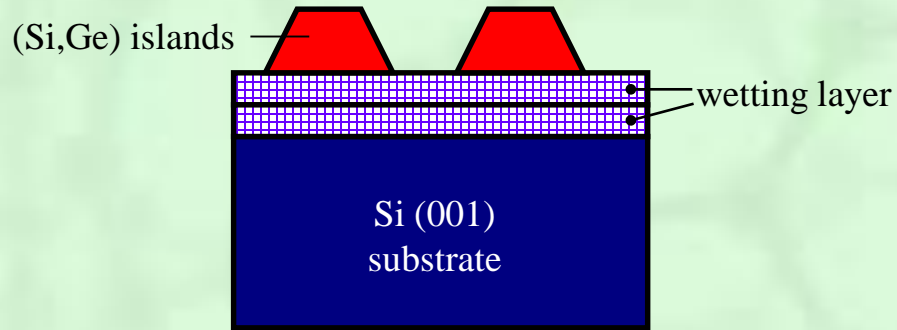
... the nano-particles
arrange themselves
symmetrically ...



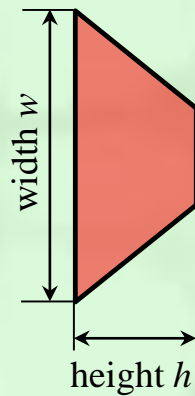
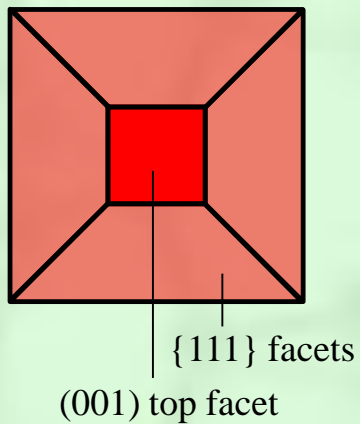
... and form
symmetrical
crystals

Motivation

Shape and geometry



Stranski-Krastanov growth (*Self-organized growth*)



Aspect ratio:
experimental:

$$A_r = w / h$$
$$A_r \approx 2.0$$

Topography by AFM

